

TEST OF T, CP, AND CPT DISCRETE SYMMETRIES VIA KAONS' TRANSITIONS AT KLOE-2*

SZYMON GAMRAT

on behalf of the KLOE-2 Collaboration

Marian Smoluchowski Institute of Physics, Jagiellonian University, Poland
szymon.gamrat@doctoral.uj.edu.pl

*Received 30 July 2024, accepted 12 October 2024,
published online 27 November 2024*

Pairs of neutral kaons produced at the DAΦNE collider allowed to perform the first model-independent direct test of T, CP, and CPT symmetries utilizing the oscillations between the flavor and CP eigenbases. The analysis of 1.7 fb^{-1} data collected in 2004–2005 in the KLOE experiment led to the determination of ratios and double ratios of kaons' decay rates, establishing a few percent precision of the measurement in a model-free manner.

DOI:10.5506/APhysPolBSupp.17.7-A4

1. Motivation of T, CP, and CPT tests

The history of discrete symmetries studies includes both direct and indirect measurement approaches. The most significant direct results include the indirect CP violation test of Cronin and Fitch [1], the P symmetry test based on ^{60}Co decays [2], the test of T symmetry done by BaBar Collaboration [3], and finally the direct CP violation measured by NA48 Collaboration and the kTeV experiment [4, 5]. While the CP violation is well established in the quark sector, in the lepton sector, can be searched for by exploiting the correlations in positronium decays, precise tests in this field have been performed recently by the J-PET Collaboration [6, 7]. The novel methods based on the kaons' transitions were proposed and used in the following studies. The model-free approach, described in [8, 9], provides a universal tool for discrete symmetries testing to complement the results in the T and CP field, and directly measure the CPT symmetry.

* Presented at the 5th Jagiellonian Symposium on *Advances in Particle Physics and Medicine*, Cracow, Poland, June 29–July 7, 2024.

2. DAΦNE collider and the KLOE experiment

DAΦNE at INFN Laboratori Nazionali di Frascati is an electron–positron collider operating on the CM energy of $\sqrt{s} = 1020$ MeV, which maximizes the probability of $\phi(1020)$ meson production [10]. The significant decay probability $\text{BR}(\phi \rightarrow K_L K_S) = (33.9 \pm 0.4)\%$ allowed to measure directly the decays of entangled K_S and K_L .

The reconstruction of charged particles was provided by the gaseous Drift Chamber (DC) with the relative momentum resolution at the 0.5% level [11]. The surrounding Electromagnetic Calorimeter (EMC) allowed for the measurement of long-living particles' energy deposition. The resolutions of energy $\sigma_E/E = 0.057/\sqrt{E(\text{GeV})}$, cluster time $\sigma_t = 54 \text{ ps}/\sqrt{E(\text{GeV})} \oplus 100 \text{ ps}$, position along $\sigma_{\parallel} = 1.4 \text{ cm}/\sqrt{E(\text{GeV})}$, and perpendicular to the fibers $\sigma_{\perp} = 1.3 \text{ cm}$ provide a high-quality reconstruction of the decay vertices in an event [12].

3. Ratios and double ratios of kaons' transition probabilities

The measurement approach was based on the existence of flavor and CP operator eigenbases denoted via $\{K^0, \bar{K}^0\}$ and $\{K_+, K_-\}$, respectively. Thus, the initial state of kaons' pair can be written as

$$|i\rangle = \frac{1}{\sqrt{2}} (|K^0\rangle |\bar{K}^0\rangle - |\bar{K}^0\rangle |K^0\rangle) = \frac{1}{\sqrt{2}} (|K_+\rangle |K_-\rangle - |K_-\rangle |K_+\rangle) . \quad (3.1)$$

3.1. Flavor and CP decay channels

To recognize the flavor and CP eigenstates, their specific decay channels are used. In the following studies, the $\Delta S = \Delta Q$ rule was assumed, so the $|K^0\rangle$ can only decay into $\pi^- l^+ \nu$ and $|\bar{K}^0\rangle$ into $\pi^+ l^- \nu$, where $l = e, \mu$ — the state was recognized by the charge of a lepton. In the second case, the direct CP and CPT violations are negligible, so for the exact CP-even state $|K_+\rangle$, the decay into $\pi^+ \pi^-$ was allowed, while the CP-odd state $|K_-\rangle$ can decay only into $3\pi^0$.

3.2. Flavor–CP transitions and the decay probability ratios

The oscillations in the quark sector lead to the transitions of kaon states between the flavor and CP bases. Assuming that the Δt was system's evolution time, the model-free probability ratios are constructed for the T test

$$R_{1,T}(\Delta t) = P [K_+(0) \rightarrow \bar{K}^0(\Delta t)] / P [\bar{K}^0(0) \rightarrow K_+(\Delta t)] ,$$

$$\begin{aligned}
 R_{2,T}(\Delta t) &= P [K^0(0) \rightarrow K_-(\Delta t)] / P [K_-(0) \rightarrow K^0(\Delta t)] , \\
 R_{3,T}(\Delta t) &= P [K_+(0) \rightarrow K^0(\Delta t)] / P [K^0(0) \rightarrow K_+(\Delta t)] , \\
 R_{4,T}(\Delta t) &= P [\bar{K}^0(0) \rightarrow K_-(\Delta t)] / P [K_-(0) \rightarrow \bar{K}^0(\Delta t)] , \quad (3.2)
 \end{aligned}$$

for the CP test

$$\begin{aligned}
 R_{1,CP}(\Delta t) &= P [K_+(0) \rightarrow \bar{K}^0(\Delta t)] / P [K_+(0) \rightarrow K^0(\Delta t)] , \\
 R_{2,CP}(\Delta t) &= P [K^0(0) \rightarrow K_-(\Delta t)] / P [\bar{K}^0(0) \rightarrow K_-(\Delta t)] , \\
 R_{3,CP}(\Delta t) &= P [\bar{K}^0(0) \rightarrow K_+(\Delta t)] / P [K^0(0) \rightarrow K_+(\Delta t)] , \\
 R_{4,CP}(\Delta t) &= P [K_-(0) \rightarrow K^0(\Delta t)] / P [K_-(0) \rightarrow \bar{K}^0(\Delta t)] , \quad (3.3)
 \end{aligned}$$

and for the CPT test

$$\begin{aligned}
 R_{1,CPT}(\Delta t) &= P [K_+(0) \rightarrow \bar{K}^0(\Delta t)] / P [K^0(0) \rightarrow K_+(\Delta t)] , \\
 R_{2,CPT}(\Delta t) &= P [K^0(0) \rightarrow K_-(\Delta t)] / P [K_-(0) \rightarrow \bar{K}^0(\Delta t)] , \\
 R_{3,CPT}(\Delta t) &= P [K_+(0) \rightarrow K^0(\Delta t)] / P [\bar{K}^0(0) \rightarrow K_+(\Delta t)] , \\
 R_{4,CPT}(\Delta t) &= P [\bar{K}^0(0) \rightarrow K_-(\Delta t)] / P [K_-(0) \rightarrow K^0(\Delta t)] . \quad (3.4)
 \end{aligned}$$

For the KLOE experiment, only the ratios with subscripts 2 and 4 are measurable. If symmetry is conserved, the corresponding ratios should be equal to unity. To compare the ratios for the opposite strangeness, the double ratios $R_{2,T}(\Delta t)/R_{4,T}(\Delta t)$ and $R_{2,CPT}(\Delta t)/R_{4,CPT}(\Delta t)$ are additionally measured. Identification of the kaon states utilizing the $\pi^-l^+\nu$, $\pi^+l^-\nu$, $\pi^+\pi^-$, and $3\pi^0$ leads finally to the measurement of T , CP , and CPT symmetries.

4. Analysis methods

As the entangled $K_S K_L$ pairs are produced in the signal events, the time ordering was introduced: K_1 stands for the early decaying kaon, while K_2 for the late decaying one. The theoretical and experimentally measurable probability ratios are connected with the $D = (0.5076 \pm 0.0059) \times 10^{-3}$ factor expressed by [13]

$$D = \frac{\text{BR}(K_L \rightarrow 3\pi^0) \Gamma_L}{\text{BR}(K_S \rightarrow \pi^+\pi^-) \Gamma_S} , \quad (4.1)$$

where $\Gamma_{S(L)}$ are the decay widths of $K_{S(L)}$. The parameters were provided by KLOE with the highest known precision [14]. The analysis flow is described in detail in the following subsections.

4.1. Flavor-states transitions into CP-odd state

Identification of $K^0 \rightarrow K_-$ and $\bar{K}^0 \rightarrow K_-$ was synonymous to the selection of $K_1 \rightarrow \pi^\pm e^\mp \nu$ and $K_2 \rightarrow 3\pi^0$. Due to the entanglement, if $K_1 \rightarrow \pi^\pm e^\mp \nu$ is observed, then K_1 is in the $|\bar{K}^0\rangle$ or $|K^0\rangle$ state, so K_2 is in the opposite state $|K^0\rangle$ or $|\bar{K}^0\rangle$, respectively. After the time Δt , the $K_2 \rightarrow 3\pi^0$ is observed, so the transition $K^0 \rightarrow K_-$ or $\bar{K}^0 \rightarrow K_-$ is identified.

Firstly, the $3\pi^0 \rightarrow 6\gamma$ decays are reconstructed utilizing the trilateration method [15]. The path length of a photon from $K \rightarrow 3\pi^0 \rightarrow 6\gamma$, which reached the calorimeter, can be considered as the radius of a sphere centered at its collision point. The trilateration method was equivalent to the geometrical determination of the intersection point of these spheres. Formally, only 4 photons are needed to determine the neutral vertex, however, the inclusion of additional 2γ improves the final resolutions of kaon path length and time of flight (measured in proper time) to 1.3 cm and $1.6 \tau_S$ respectively. At this point, late kaon decays are in 98% dominated by the $3\pi^0$ states.

For $K_1 \rightarrow \pi^\pm e^\mp \nu$ preselection, the cylindrical region of spatial acceptance (fiducial volume) with the transverse radius $\rho < 3$ cm and $|z| < 4.5$ cm of the charged vertex with two assigned DC tracks was used. Initially, the main background component $K_1 \rightarrow \pi^+\pi^-$ was reduced by the invariant mass condition $m_{\pi\pi} < 490$ MeV. The further rejection was done by the time-of-flight (TOF) analysis of tracks that hit the EMC — examples of the used distributions are shown in Fig. 1. The geometrical cuts used to select the proper timing for the $K_1 \rightarrow \pi^\pm e^\mp \nu$ channel leave the sample at the 88% purity level. The remaining background originates mainly from the

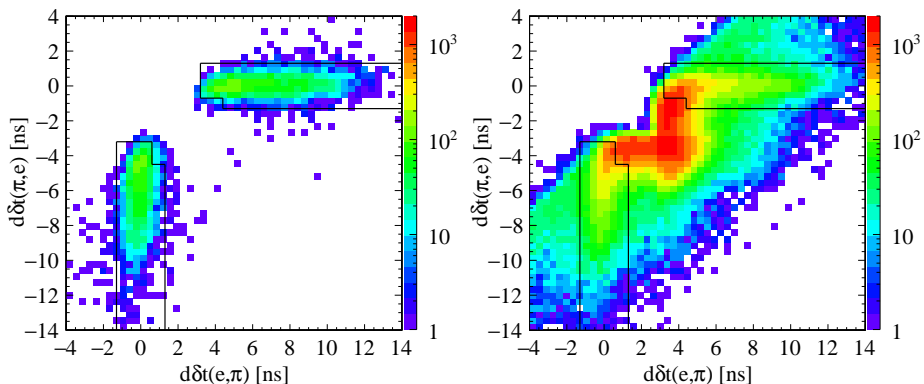


Fig. 1. Example of the TOF geometrical cut used to classify the charged particles' tracks as π or e for signal events (left) and the entire data set (right). The events outside the black outlines are rejected. Figure adapted from Ref. [13].

misidentified charged tracks — the additional classification was done via the Multilayer Perceptron model available in the TMVA package, which was the last selection step. The overall purity for the $K_1 K_2 \rightarrow (\pi^\pm e^\mp \nu)(3\pi^0)$ sample reaches 96%.

4.2. Flavor-states transitions into CP -even state

The transitions $K_- \rightarrow K^0$ and $K_- \rightarrow \bar{K}^0$ are found by the selection of $K_1 \rightarrow \pi^+ \pi^-$ and $K_2 \rightarrow \pi^\pm e^\mp \nu$. The identification is similar to the previous subsection — if $K_1 \rightarrow \pi^+ \pi^-$ is observed, then K_1 is in the $|K_+\rangle$ state. K_2 is in the opposite state $|K_-\rangle$ and if after the time Δt the $K_2 \rightarrow \pi^\pm e^\mp \nu$ is observed, the transition $K_- \rightarrow \bar{K}^0$ or $K_- \rightarrow K^0$ is identified. Due to the presence of two different charged channels, the fiducial volume in this case was increased to $\rho < 15$ cm and $|z| < 10$ cm around the interaction point.

To select $K_2 \rightarrow \pi^\pm e^\mp \nu$, all the vertices in the fiducial volume are considered, excluding those identified earlier as the $\pi^+ \pi^-$ decays. The first step to find the semileptonic decays was the determination of the invariant masses of the positive and negative tracks with m_\pm . The m_\pm should correspond to the e^\pm mass — the events, which do not fulfill $m_+^2 + m_-^2 > 0.015 \text{ GeV}^2$ are rejected. The final selection was based on the TOF conditions described in the previous subsection. The proposed analysis method leaves the $K_1 K_2 \rightarrow (\pi^+ \pi^-)(\pi^\pm e^\mp \nu)$ sample at the overall 99% purity level.

4.3. Efficiency estimation

The total efficiency consists of two components: ε_{TEC} dependent on triggers, background filters and stream classification algorithms, and $\varepsilon(\Delta t)$, which was the result of the adopted selection methods and cuts.

The first contribution was estimated basing on the sample of minimum bias events ($\sim 15\%$ of ϕ events), which were preserved from the initial filtering and classification to get the impact of applied triggers.

The $\varepsilon(\Delta t)$ was evaluated with Monte Carlo and corrected with the control samples selected from data. For the correction, $K_1 K_2 \rightarrow (\pi^+ \pi^-)(3\pi^0)$ and $K_1 K_2 \rightarrow (\pi^0 \pi^0)(\pi^\pm e^\mp \nu)$ decays were analyzed. $K_2 \rightarrow 3\pi^0$ and $K_2 \rightarrow \pi^\pm e^\mp \nu$ were selected using the conditions described in Subsections 4.1 and 4.2, but firstly they were tagged with $K_1 \rightarrow \pi^+ \pi^-$ and $K_1 \rightarrow \pi^0 \pi^0$, respectively. Finally, the efficiency correction was evaluated by the comparison of Monte Carlo and data-based efficiencies of tagged samples, and was applied to the final measurement [13].

5. Result and outlook

The final measured ratios sensitive to potential symmetries' violation are gathered in Fig. 2. The results are compared to expected values (dashed lines) assuming CPT invariance, $\Delta S = \Delta Q$ rule [8] (K^0 and \bar{K}^0 can be identified by the charge of lepton in the final state) and T violation extracted from CP violation mixing [16]. The first direct, most precise kaon-related measurement of T, CP, and CPT demonstrates the conservation of T and CPT, while the CP symmetry, as expected, was violated. The last term in Eqs. (5.1)–(5.4) is the contribution to the uncertainty due to the D factor. The main contribution to the systematic errors for each determined ratio comprises of the choice of the Δt bin width, the fit range, and the $e/\pi/\mu$ classification methods sensitivity. The precision of T and CPT single ratio tests reaches 2.5%, while for the double ratios, it was 3.5%. Finally, CP measurement relative uncertainty stays at the level of 0.13%.

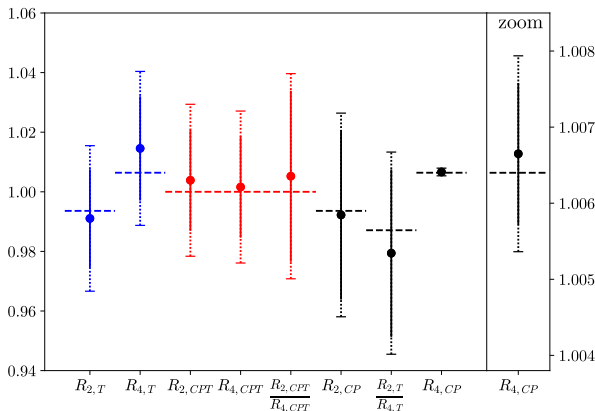


Fig. 2. Results of the T, CP, CPT measurement. Figure adapted from Ref. [13]. The solid error bars describe statistical uncertainties, while the dotted ones are the total errors.

$$R_{2,T} = 0.991 \pm 0.017_{\text{stat}} \pm 0.014_{\text{syst}} \pm 0.012_D, \quad (5.1)$$

$$R_{4,T} = 1.015 \pm 0.018_{\text{stat}} \pm 0.015_{\text{syst}} \pm 0.012_D, \quad (5.2)$$

$$R_{2,CPT} = 1.004 \pm 0.017_{\text{stat}} \pm 0.014_{\text{syst}} \pm 0.012_D, \quad (5.3)$$

$$R_{4,CPT} = 1.002 \pm 0.017_{\text{stat}} \pm 0.015_{\text{syst}} \pm 0.012_D, \quad (5.4)$$

$$R_{2,CP} = 0.992 \pm 0.028_{\text{stat}} \pm 0.019_{\text{syst}}, \quad (5.5)$$

$$R_{4,CP} = 1.00665 \pm 0.00093_{\text{stat}} \pm 0.00089_{\text{syst}}, \quad (5.6)$$

$$R_{2,T}/R_{4,T} = 0.979 \pm 0.028_{\text{stat}} \pm 0.019_{\text{syst}}, \quad (5.7)$$

$$R_{2,CPT}/R_{4,CPT} = 1.005 \pm 0.029_{\text{stat}} \pm 0.019_{\text{syst}}. \quad (5.8)$$

The 2 times greater integrated luminosity collected by the KLOE-2 Collaboration allows for improving the result in the future. The KLOE-2 detector upgraded with the CGEM Inner Tracker [17] provides access to charged kaon decays, which do not reach DC. It can lead to the improvement of measurement's precision in the future.

I warmly thank Prof. Paweł Moskal and Prof. Ewa Stępień for admitting the poster for the 5th Jagiellonian Symposium on Advances in Particle Physics and Medicine. I am very grateful to Dr. Eryk Czerwiński for his substantive help and to the colleagues at KLOE-2 for all their constructive criticism during the preparation of the article.

REFERENCES

- [1] J.H. Christenson, J.W. Cronin, V.L. Fitch, R. Turlay, *Phys. Rev. Lett.* **13**, 138 (1964).
- [2] C.S. Wu *et al.*, *Phys. Rev.* **105**, 1413 (1957).
- [3] BaBar Collaboration (J.P. Lees *et al.*), *Phys. Rev. Lett.* **109**, 211801 (2012).
- [4] NA48 Collaboration (J.R. Batley *et al.*), *Phys. Lett. B* **544**, 97 (2002).
- [5] E. Abouzaid *et al.*, *Phys. Rev. D* **83**, 092001 (2011).
- [6] P. Moskal *et al.*, *Nat. Commun.* **12**, 5658 (2021).
- [7] P. Moskal *et al.*, *Nat. Commun.* **15**, 78 (2024).
- [8] J. Bernabeu, A. Di Domenico, P. Villanueva-Perez, *Nucl. Phys. B* **868**, 102 (2013).
- [9] J. Bernabeu, A. Di Domenico, P. Villanueva-Perez, *J. High Energy Phys.* **2015**, 139 (2015).
- [10] A. Gallo *et al.*, *Conf. Proc. C* **060626**, 604 (2006), report No. SLAC-PUB-12093
- [11] M. Adinolfi *et al.*, *Nucl. Instrum. Methods Phys. Res. A* **488**, 51 (2002).
- [12] M. Adinolfi *et al.*, *Nucl. Instrum. Methods Phys. Res. A* **482**, 364 (2002).
- [13] D. Babusci *et al.*, *Phys. Lett. B* **845**, 138164 (2023).
- [14] Particle Data Group (R.L. Workman *et al.*), *Prog. Theor. Exp. Phys.* **2022**, 083C01 (2022).
- [15] A. Gajos, Ph.D. Thesis, Jagiellonian University, Faculty of Physics, Astronomy and Applied Computer Science, 2018.
- [16] Particle Data Group (P.A. Zyla *et al.*), *Prog. Theor. Exp. Phys.* **2020**, 083C01 (2020).
- [17] A. Balla *et al.*, *Nucl. Instrum. Methods Phys. Res. A* **845**, 266 (2017).